Meccanica (2011) 46:979–987
DOI 10.1007/s11012-010-9356-2

Realization of a new experimental setup for magnetostrictive actuators

Francesco A. Raffa · Paolo E. Roccato · Mauro Zucca

Received: 24 September 2009 / Accepted: 9 September 2010 / Published online: 28 September 2010

Abstract A new setup for the prospective investigation of the active damping properties of magnetostrictive (MST) actuators has been realized. A dynamical finite element analysis has been carried out to meet the design requirements concerning the eigenvalues spectra and the mode shapes of the setup: experimental and numerical results match satisfactorily. The setup has given a clear evidence of the damping capabilities of a MST actuator developed by our group and utilized as a compensator of external harmonic excitations.

Keywords Magnetostriction · Actuators · Vibrations · Damping

1 Introduction

The magnetostriction is the deformation of a body as a consequence of the modification of its magnetization state, usually due to the application of an external magnetic field. All ferromagnetic materials exhibit magnetostriction but only a limited number of materials, containing rare earth elements, are endowed with a level of magnetostriction appropriate to application purposes; they are referred to as giant MST materials. From the 1960s the ferromagnetic alloy Terfenol-D ($Tb_{0.3}Dy_{0.7}Fe_2$), developed by the Naval Ordnance Laboratory, has been extensively investigated and utilized as actuator and sensor/transducer. Nowadays other materials such as polimer-bonded Terfenol-D, Co-ferrites and Iron-Gallium alloys (Galfenol) are also available. Giant MST materials belong to the class of magnetoelastic materials and, to be effective in applications, they have to be preloaded usually by means of a set of springs. For these materials the link between the deformation and the magnetic field is in general nonlinear, exhibits hysteresis and depends on the applied preload. In turn, the mechanical preload influences also the magnetic characteristics relating the applied magnetic field, which depends on the driving current, to the material magnetization. Both effects are shown in the graphs of Fig. 1, where H and B are the magnetic field density and the magnetic flux density, respectively, while ε is the mechanical strain. The main topics concerning the giant MST materials are extensively dealt with in [1].

In spite of the difficulties related to nonlinearity and hysteresis, MST devices have proved very interesting due to the high dynamic performance of the MST materials (frequencies of the order of many kHz) and to the large forces they can exert (the compressive strength of Terfenol-D is about 700 MPa, with a standard preload of 10–15 MPa). As for the displacement obtainable through MST devices, it is related to

F.A. Raffa (✉)
Dipartimento di Meccanica, Politecnico di Torino, Corso Duca degli Abruzzi, 24, 10129 Torino, Italy
e-mail: francesco.raffa@polito.it

P.E. Roccato · M. Zucca
Divisione Elettromagnetismo, INRiM, Strada delle Cacce, 91, 10135 Torino, Italy

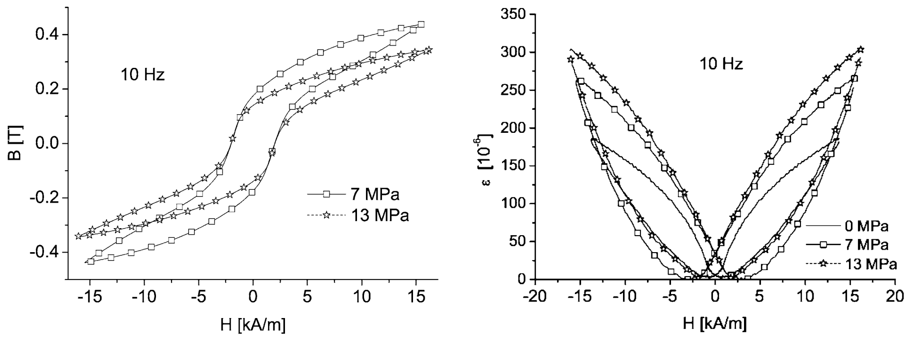

Fig. 1 Measured magnetic and magneto-mechanical characteristics of a Terfenol-D rod for various levels of the preload; the supply frequency is 10 Hz

the mechanical strain of the MST rod which varies usually between 200 ppm and 1000 ppm at the most. Thus such devices perform better in sonic applications (sonar), microactuators, sensors and active compensators of vibrations. Novel modeling approaches as those investigated in [2–16], lead to an efficient design of these devices solving the main critical aspects in the coupling between electromagnetic and mechanical requirements.

The present work has been developed in the framework of a research project focused on the active vibration compensation of modern computer numerically controlled machine tools (CNC), though one should at least mention the widespread utilization of smart materials in CNC applications also for the tools motion and positioning, as reported, e.g., in [17].

In high quality processing, CNC machining precision in milling and lathing operation is limited by the spindle vibrations whose frequencies range from a few Hz (roughing operations) to nearly 1 kHz (finishing operations). Natural candidates for the mechanical vibrations compensation are the piezoelectric (PZT) and the more recent MST actuators. On the one hand, MST devices show some advantages with respect to PZT appliances: they can exert higher forces, are less affected by electrical insulation and cooling problems and are characterized by a lower brittleness with respect to the action of lateral loads. On the other hand, MST systems are generally heavier than PZT devices due to their magnetic circuit.

As regards the compensation of mechanical vibrations of actual structures through PZT or MST devices, the incorporation of active elements is also to be mentioned for applications such as plates [18, 19], spacecraft platform [20], rotating shafts [21].

The aim of this paper is the realization of a test bench for investigating the ability of a magnetoelastic device to compensate the vibrations induced by an external forcing load applied to the bench. In an actual application this would correspond to the compensation of the vibrations produced by a spindle on its base. While the realization of setups for the characterization of the MST materials is fairly common, the design of a setup for the experimental investigation of MST devices remains, to our knowledge, an open problem. In the field of the active vibration compensation, different solutions have been proposed; for instance, in [22] two loaded actuators have been stacked one on the other, with two interposed tables for frequencies up to 5 Hz, while in [23] a beam has been constrained between two MST actuators for frequencies up to a few hundreds Hz. However, the vibrations of an actual device resemble more those of a slab than those of a beam; this is especially true for a CNC machine tool whose spindle is usually placed on a plate. Moreover, the actuator has to continuously compensate structural vibrations up to 1 kHz. In view of the above considerations, here a structure shaped as a bench is proposed. Such structural solution has two main features: (i) it makes available a wide range of loads on the actuators, (ii) the natural frequencies can be changed upon modifying the material and the geometry (width and thickness) of the upper slab. In Fig. 2 the three abovementioned solutions are schematically drawn.

2 Setup design and dynamical FEM analysis

The setup has been realized resorting to both basic principles of mechanical design and an extensive dynamical FEM analysis, the latter playing the major

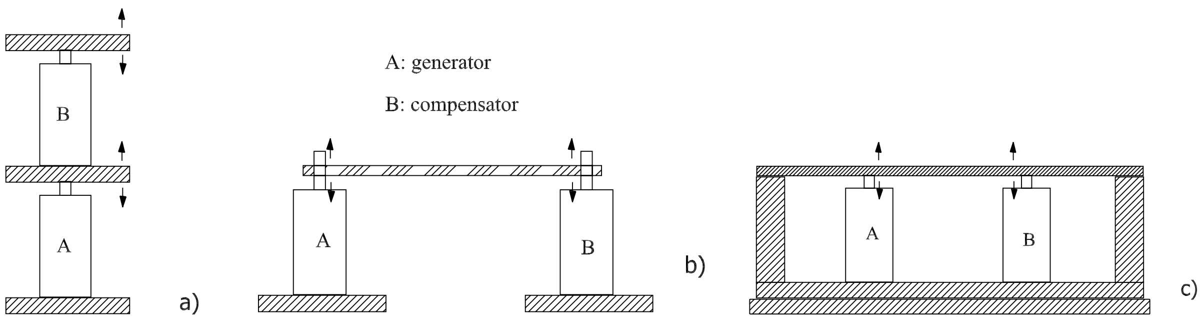

Fig. 2 Schemes of test benches for the performance analysis of a MST damper actuator: (**a**) as in [22], (**b**) as in [23], (**c**) present work

role in the final choice. The following design criteria were to be satisfied:

- In the frequency range of interest from 0 Hz to 1 kHz an optimal distribution of natural frequencies and modes is required. This means that the setup should exhibit regularly spaced frequencies and geometrically simple and well-defined mode shapes; in particular, mixed modes, i.e., modes with a relevant flexural contribution of the columns, must be avoided since they induce lateral loads on the magnetostrictive actuator, which is designed to exert only axial forces;
- an easy access to the actuators must be guaranteed;
- a stiff and reliable mechanical connection to the breadboard on which the proposed test bench is installed must be realized.

To meet the above requirements we devised a frame consisting of two steel columns having dimensions in mm $50 \times 125 \times 200$ whose bottom sides are connected to a steel base (dimensions in mm $650 \times 250 \times 20$) which, in turn, is attached to the breadboard. On the columns upper sides two aluminum plates can be fixed, their dimensions in mm being $500 \times 125 \times 15$ (plate I) and $500 \times 80 \times 5$ (plate II). The threaded connections at the columns/plates and base/breadboard interfaces for the setup configuration with plate I are specified in Fig. 3. The total weight of the setup is 319 N and 335 N depending on which plate one utilizes.

The geometry and the material properties of both plates and columns were fixed through a preliminary dynamical FEM analysis of several alternative solutions, all based on the common feature of utilizing well known vibrating bodies (the plates) dynamically uncoupled with respect to the vertical supports on which they are fixed (the columns). In addition to being uncoupled with respect to the columns, the plate modes in the frequency experimental range should be as much as possible 'beam-like' modes characterized by the flexural vibration of the plate along its major dimension: indeed, this simplifies the selection of the appropriate points for the application of both actuators.

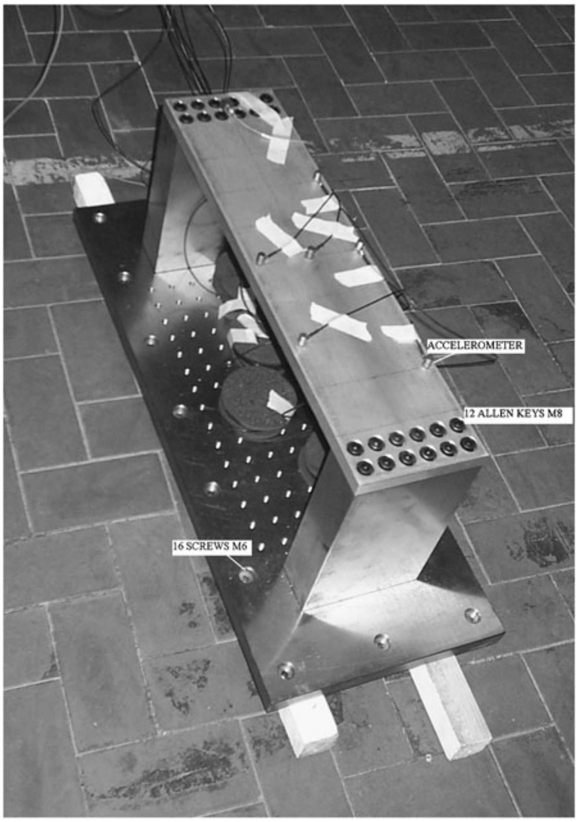

Fig. 3 Setup instrumented for dynamical testing (configuration with plate I)

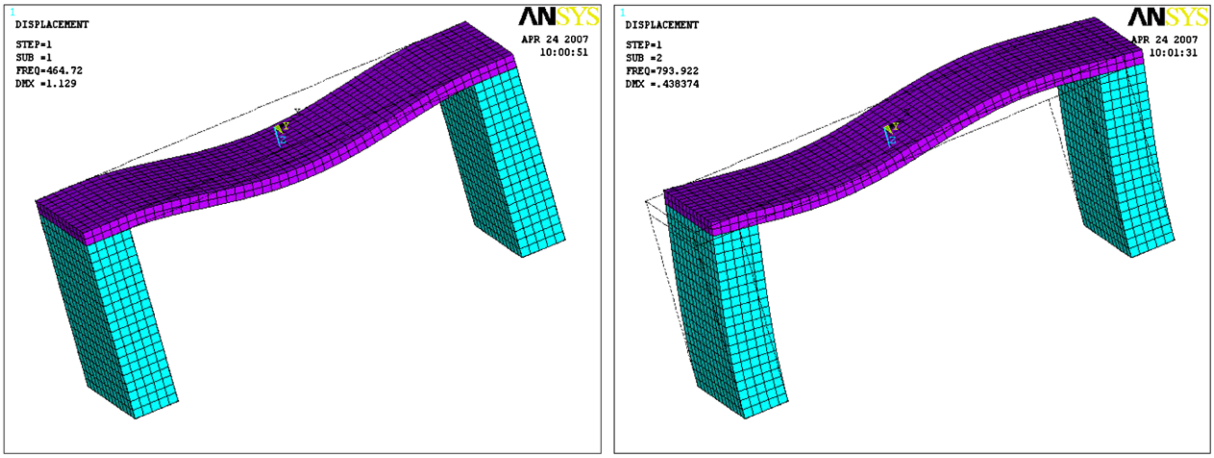

Fig. 4 The setup first (464 Hz) and second (793 Hz) mode (configuration with plate I)

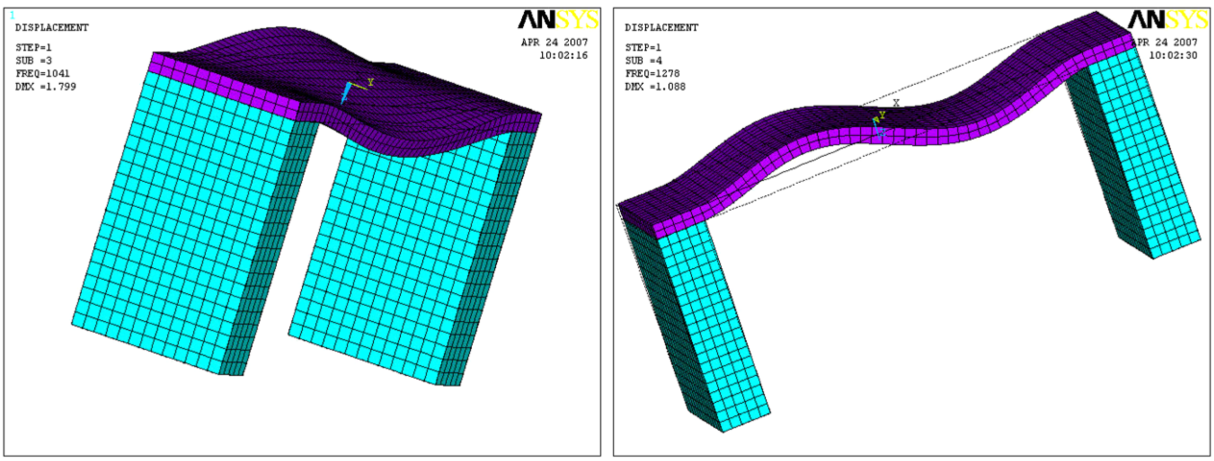

Fig. 5 The setup third (1040 Hz) and fourth (1277 Hz) mode (configuration with plate I)

The free response of the setup was calculated resorting to three-dimensional FEM models [24] defined utilizing the numerical convergence analysis of the first six natural frequencies of plate II; clamped constraints were imposed at the bottom of the columns in view of the stiff fastening condition at the base/columns interface. The following values for the mechanical properties of steel and aluminum were utilized: Young's modulus 200 GPa and 70 GPa, material density 7800 $\mathrm{kg\,m^{-3}}$ and 2700 $\mathrm{kg\,m^{-3}}$, Poisson's coefficient 0.3 for both.

There are four and six natural modes lying in the experimental range from 0 Hz to approximately 1 kHz for the setup with plate I and II, respectively. On examination of the numerical results one finds that, for plate I, the first mode shape (464 Hz) fits the requirements for the forced response test, as the plate manifestly vibrates in a beam-like mode with the columns unaffected, while the second mode (793 Hz) is a mixed one, with the columns partecipating to the overall shape more significantly than the plate, as shown in Fig. 4. The third mode (1040 Hz), characterized by the torsion-like deformation of the upper plate with the columns unaffected, and the fourth, beam-like, mode (1277 Hz) are shown in Fig. 5; notice that in the third mode the experimental conditions would prove somehow cumbersome. Our conclusion is that both the second and the third mode cannot be favourably considered for carrying out the forced response test.

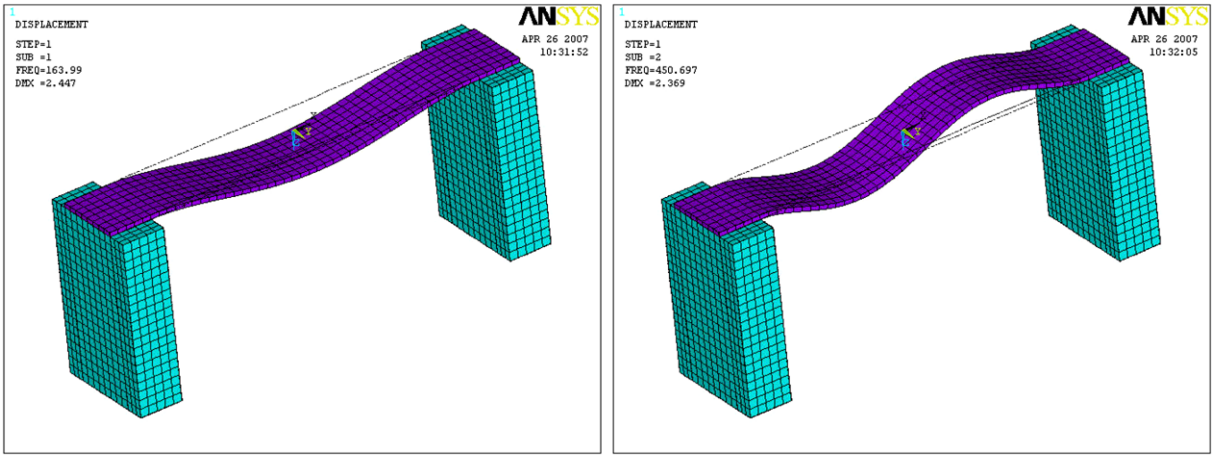

Fig. 6 The setup first (164 Hz) and second (450 Hz) mode (configuration with plate II)

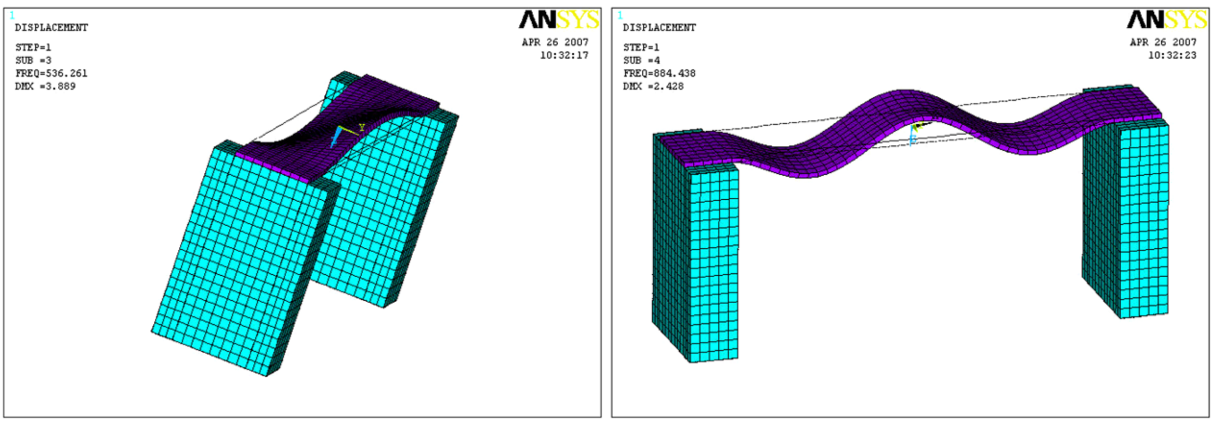

Fig. 7 The setup third (536 Hz) and fourth (884 Hz) mode (configuration with plate II)

For the setup configuration with plate II the FEM results show that the modes first (164 Hz), second (450 Hz) and fourth (884 Hz) possess the required characteristics: their frequencies are nearly regularly spaced while the plate vibrations have beam-like shapes of increasing order with the columns not involved in the overall shape, as illustrated in Figs. 6 and 7. On the contrary, the modes third (536 Hz) and sixth (1107 Hz), shown in Figs. 7 and 8, exhibit a plate torsional component of increasing complexity with the columns unaffected, while the fifth one (947 Hz) in Fig. 8 is mixed, with a major columns contribution to the mode.

The above considerations can be summarized as follows: the setup configuration with plate II realizes the best distribution of both natural frequencies and mode shapes, with three well defined beam-like modes which can be quite easily selected according to the kind of forced response test one has to perform on the actuators. Nevertheless, also the stiffer configuration with plate I, where only the first mode at 464 Hz can be appropriately utilized, has been realized in order to prevent prospective difficulties related to the comparatively large flexibility of plate II.

3 Experimental validation of the FEM models

To validate the above FEM models, the experimental free response of the setup was investigated through modal testing procedure. The view of the instrumented

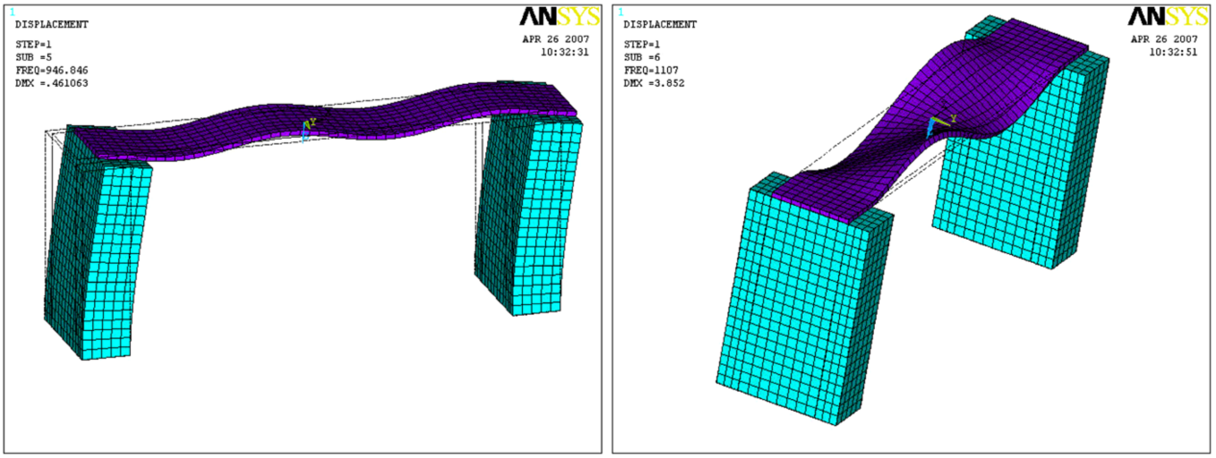

Fig. 8 The setup fifth (947 Hz) and sixth (1107 Hz) mode (configuration with plate II)

Table 1 FEM and experimental results for setup with plate I

Mode	1st	2nd	3rd	4th
ω_r [Hz] FEM	464	793	1040	1277
ω_r [Hz] exp	448	–	1011	1205
ζ_r exp	0.490	–	0.311	0.399

Table 2 FEM and experimental results for setup with plate II

Mode	1st	2nd	3rd	4th	5th	6th
ω_r [Hz] FEM	164	450	536	884	947	1107
ω_r [Hz] exp	145	410	481	794	–	1014
ζ_r exp	0.603	1.024	1.318	0.846	–	1.154

setup in Fig. 3 shows that seven accelerometers were applied to the upper plate. One of them is placed at the middle section of one of the columns, where vertical accelerations are expected to be quite low, so that its sensitivity (9.86 mV/ms^{-2}) is nearly ten times larger than the average sensitivity of the others.

The measured modal parameters are natural frequencies ω_r, natural modes and dimensionless damping ζ_r. The numerical and experimental values of ω_r and the experimental mean values of ζ_r are reported in Tables 1 and 2 for plate I and plate II, respectively, with reference to the experimental range of frequencies: FEM analysis and modal testing compare favorably.

Notice that the mixed modes (the second and the fifth one for the setup configurations with plate I and plate II, respectively), characterized by major columns oscillations, were not detected by the accelerometers attached to the plates. We verified that even exciting the setup in the direction of the column mode does not result into a significant transverse motion of the plates. This implies that the above modes do not affect the experimental conditions: indeed, during the tests both the excitation of the plates and the compensation of their oscillations take place along the transverse direction of the plates. Also the graphs of the power spectral density (PSD) in Fig. 9 support this point of view: they show the response from accelerometer n. 3

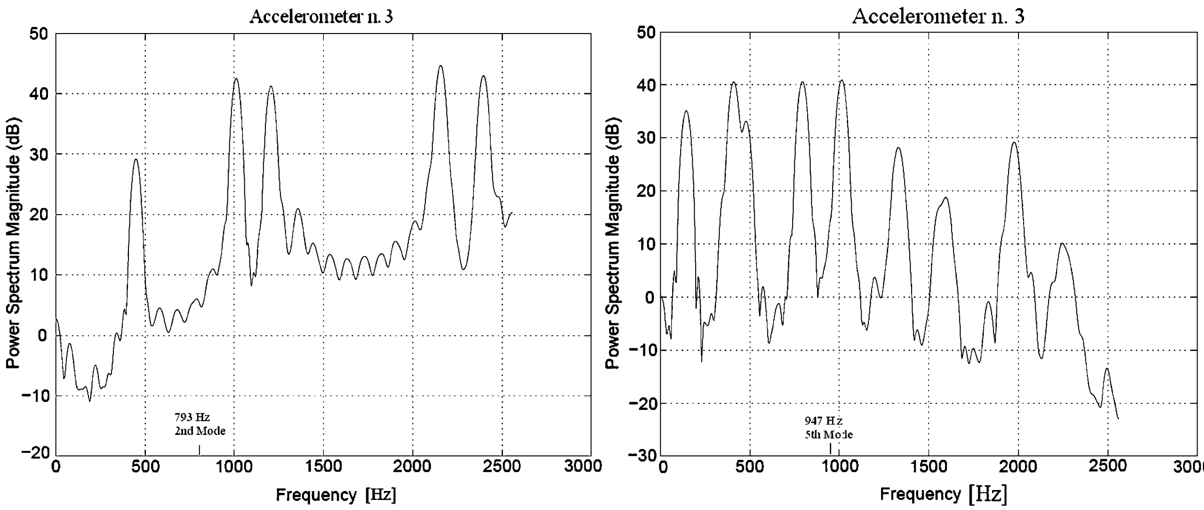

Fig. 9 PSD from accelerometer n. 3 for the setup configurations with plate I (*left*) and plate II (*right*)

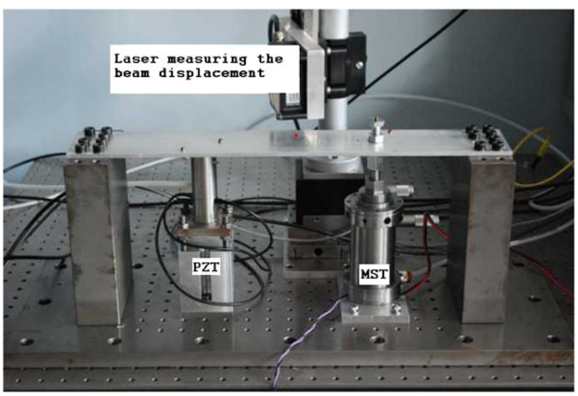

Fig. 10 Tests of vibrations compensation (configuration with plate II)

which, for both plates, is the one in the low right position in Fig. 3.

4 Preliminary damping tests

The setup was tested for a first investigation of the damping capability of a MST actuator realized and characterized by our group [8] with respect to the lateral vibrations of the upper plate. The experimental conditions are illustrated in Fig. 10, which shows that the MST actuator is linked to the upper plate (plate II in the actual configuration) through a threaded connection, while a PZT actuator (Physik Instrumente mod. P-239k166) is utilized to apply a harmonic forcing displacement to the plate. The actuators, which are voltage-driven, are located symmetrically on the plate at a distance of 100 mm from the columns.

Notice that here both the PZT and the MST actuators are considered as generators of time-varying (specifically, harmonic) external actions applied to the test bench.

The amplitude of the output signal of the PZT can be regulated over a range of the applied voltage up to 10 V. The PZT displacement constant is equal to 6 μm/V, while the MST one is equal to 12 μm/A (0.73 μm/V at 200 Hz).

As for the MST, the amplitude and the phase of the signal are regulated so that the plate vibrations can be effectively compensated. The displacement at any selected points of the plate is measured through a laser system ($\mu\epsilon$ mod. optNCDT).

Figures 11 and 12 give the experimental lateral displacements at the point located in the upper right corner of the plate at 20 mm from both the axes of symmetry of the plate, for forcing frequencies of 200 Hz and 510 Hz, respectively; as reported in Table 2, the latter value is close to a resonance condition of the plate. In both figures the graphs of the driving voltages of the actuators are given and the MST signal phases corresponding to the largest reduction of the plate vibrations are also reported. The compensation of the plate vibrations obtained through the MST actuator under sinusoidal excitation, is nearly 70% and 95% at 200 Hz and 510 Hz, respectively, proving very satisfactory particularly in the resonance condition. Simi-

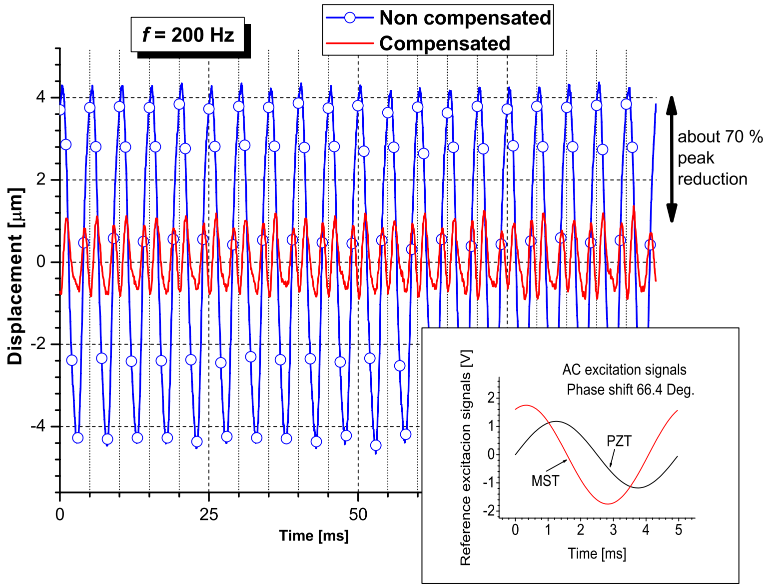

Fig. 11 Measured compensation (setup with plate II, forcing frequency 200 Hz)

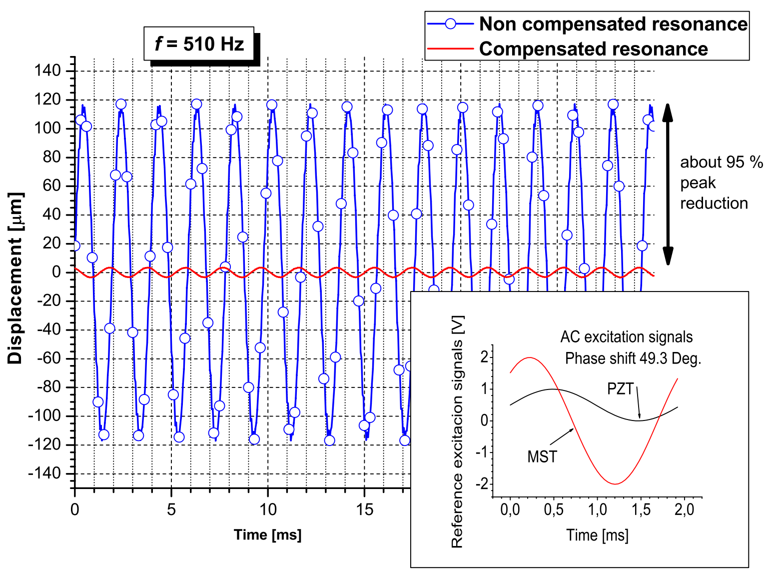

Fig. 12 Measured compensation (setup with plate II, forcing frequency 510 Hz)

lar results were obtained measuring the displacements of other points placed at both symmetrical and unsymmetrical locations of the plate. It is worth mentioning that in [23], under the same excitation conditions, a vibrations amplitude reduction of about 80% and 90% at 98 Hz and 387 Hz is reported, while in [22], where the single forcing frequency of 5 Hz is considered, the amplitude reduction is as high as 98%.

5 Concluding remarks

The main points of our investigation can be summarized as follows. A new setup has been realized, which meets all the criteria for the experimental analysis of the performance of magnetostrictive actuators in the field of the active damping of mechanical vibrations. Such result has been obtained through an extensive dynamical FEM analysis to identify the geometrical and material properties of the various structural members, i.e., plates, columns, base. The experimental results concerning the free response of the proposed setup have validated both the mechanical design and the numerical analysis.

Furthermore, the setup has been tested utilizing the PZT and the MST actuators of Fig. 10 as generators of the harmonic excitation and vibrations compensator, respectively. The preliminary experimental results obtained in this work appear to be very promising in view of the realization of an active damping of mechanical vibrations with the MST actuator working appropriately as a control device. Such realization is currently investigated.

Acknowledgements This work is part of the research activity performed in the framework of the research project MAGDAMP (Magnetostrictively actuated platform for milling-induced vibration damping) financed by Regione Piemonte, Italy.

References

1. Engdahl G (2000) Handbook of giant magnetostrictive materials. Academic Press, San Diego
2. Sablik MJ, Jiles DC (1993) Coupled magnetoelastic theory of magnetic and magnetostrictive hysteresis. IEEE Trans Magn 29:2113–2123
3. Jiles DC, Lo CCH (2003) The role of new materials in the development of magnetic sensors and actuators. Sens Actuators A 106:3–7
4. Park Y-W, Kim D-Y (2004) Development of a magnetostrictive microactuator. J Magn Magn Mater 272–274:e1765–e1766
5. Davino D, Natale C, Pirozzi S, Visone C (2004) Rate-dependent losses modeling for magnetostrictive actuators. J Magn Magn Mater 272–276:e1781–e1782
6. Bottauscio O, Chiampi M, Lovisolo A, Roccato PE, Zucca M (2008) Dynamic modeling and experimental analysis of Terfenol-D rods for magnetostrictive actuators. J Appl Phys 103:07F121-1/3
7. Olabi AG, Grunwald A (2008) Design and application of magnetostrictive materials. Mater Des 29:469–483
8. Zucca M, Roccato PE, Bottauscio O, Beatrice C (2010) Analysis of losses in a magnetostrictive device under dynamic supply. IEEE Trans Magn 46:183–186
9. Stuebner M, Atulasimha J, Smith RC (2009) Quantification of hysteresis and nonlinear effects on the frequency response of ferroelectric and ferromagnetic materials. Smart Mater Struct 18:104019
10. Graham FC, Mudivarthi C, Datta S, Flatau AB (2009) Modeling of a Galfenol transducer using the bidirectionally coupled magnetoelastic model. Smart Mater Struct 18:104013
11. Pèrez-Aparicio JL, Sosa H (2004) A continuum three-dimensional, fully coupled, dynamic nonlinear finite element formulation for magnetostrictive materials. Smart Mater Struct 13:493–502
12. Bottauscio O, Lovisolo A, Roccato PE, Zucca M, Sasso C, Bonin R (2008) Modeling and experimental analysis of magnetostrictive devices: from the material characterization to their dynamic behaviour. IEEE Trans Magn 44:3009–3012
13. Sarawate NN, Dapino MJ (2008) A dynamic actuation model for magnetostrictive materials. Smart Mater Struct 17:065013
14. Kaltenbacher M, Meiler M, Ertl M (2009) Physical modeling and numerical computation of magnetostriction. COMPEL 28:819–832
15. Davino D, Giustiniani A, Visone C (2009) Experimental properties of an efficient stress-dependent magnetostriction model. J Appl Phys 105:07D512
16. Bottauscio O, Roccato PE, Zucca M (2010) Modeling the dynamic behavior of magnetostrictive actuators. IEEE Trans Magn 46:3022–3028
17. Castillo-Castaneda E, Okazaki Y (2009) Reference model control for improving motion accuracy of a micro lathe. Meccanica 44:457–464
18. Gardonio P, Aoki Y, Elliott SJ (2010) A smart panel with active damping wedges along the perimeter. Smart Mater Struct 19:065033
19. Kumar JS, Ganesan N, Swarnamani S, Padmanabhan (2004) Active control of simply supported plates with a magnetostrictive layer. Smart Mater Struct 13:487–492
20. Kamesh D, Pandiyan R, Ghosal A (2010) Modeling, design and analysis of low frequency platform for attenuating micro-vibration in spacecraft. J Sound Vib 329:3431–3450
21. Przybylowicz PM (2003) Active stabilization of a rotating shaft transmitting static torque. Meccanica 38:763–770
22. Jenner AG, Greenough RD, Allwood D, Wilkinson AJ (1994) Control of Terfenol-D under load. J Appl Phys 76:7160–7162
23. Moon SJ, Lim CW, Kim BH, Park Y (2007) Structural vibration control using linear magnetostrictive actuators. J Sound Vib 302:875–891, and references therein
24. ANSYS, Inc Software Products, release 10.0